Theor Chem Acc (2006) 116: 456–461
DOI 10.1007/s00214-006-0098-0

REGULAR ARTICLE

Michele Pavone · Orlando Crescenzi
Giovanni Morelli · Nadia Rega · Vincenzo Barone

Solvent effects on the UV (n $\rightarrow \pi^*$) and NMR (^{17}O) spectra of acetone in aqueous solution: development and validation of a modified AMBER force field for an integrated MD/DFT/PCM approach

Received: 25 November 2004 / Accepted: 5 April 2005 / Published online: 22 February 2006

Abstract A modified AMBER force field has been developed and used to compute UV and NMR spectra of acetone in aqueous solution by an integrated computational tool rooted in the density functional theory, the polarizable continuum model, and classical molecular dynamics. The results show that, provided that classical force fields are carefully reparameterized and validated, they can be part of a robust and effective approach, which can be used also by non-specialists and provides a general and powerful complement to experimental techniques.

Keywords Solvent shifts · Spectroscopic properties · Molecular dynamics · Density functionals · Continuum solvent models

1 Introduction

The development of effective implementations of methods rooted in the density functional theory (DFT) and its time dependent extension (TD–DFT) [1–7] allows the computation of spectroscopic parameters reliable enough to aid/support the interpretation of experimental data for medium-size molecules in the gas phase. In particular, TD–DFT gives access to electronic excitation energies [5–7], whereas the gauge-including atomic orbitals (GIAO) formalism [8–10], combined with a DFT approach, has proved to be particularly effective in reproducing NMR chemical shifts [11–13]. Furthermore, ab-initio molecular dynamics (AIMD) [14,15] or effective vibrational treatments beyond the harmonic approximation [16] can be used to take vibrational averaging effects into proper account [17,18].

However, the vast majority of experimental NMR and UV spectra are actually recorded in solution and their computation calls for the proper treatment of many subtle effects induced by the complex chemical environment (e.g. the solvent) [19–21]. Even if last generation continuum solvent models [19–26] provide a number of interesting results, they are not free from difficulties for hydrogen bonding solvents (in particular water) and cannot take into full account subtle dynamical effects [27–29]. At the other extreme, AIMD [14,15] is becoming increasingly popular despite its huge computational requirements. We are developing an integrated approach in which selected frames from molecular dynamics simulations are used to compute averaged molecular properties; for the selected frame, a discrete-continuum solvent model is employed, in which a reduced number of explicit solvent molecules is treated, together with the solute, at the quantum mechanical level to correctly reproduce specific effects, whereas the polarizable continuum model (PCM) is used to introduce bulk solvent effects [30–32]. The results of such an approach seem very promising, but depend of course on the quality of the dynamical simulation. On the one hand, AIMD simulations can sample very short time intervals, so that their convergence to equilibrium values is questionable. On the other hand, in semiempirical molecular dynamics (SMD) simulations, standard force fields are often not sufficiently accurate in the present context, since some spectroscopic parameters are quite sensitive to the precise geometrical features not only of the core molecular system, but also of the embedding chemical environment. A possible solution is to perform AIMD simulations for prototypical systems, and to use these results to parameterize improved classical force fields; these could then be effectively used to perform longer simulations, hopefully leading to converged equilibrium values, as well as to study larger molecular systems containing the reparameterized functional group. As a first step in this direction, we have considered solvent effects on the $n \rightarrow \pi^*$ electronic transition energy and on the ^{17}O nuclear magnetic shielding of the carbonyl group of the acetone molecule in aqueous solution. Acetone was chosen as a suitable benchmark in view of its relatively high polarity and the availability of accurate experimental [33–38] and computational [30–32,39–42] data. Of course, the system is by

M. Pavone · O. Crescenzi · G. Morelli · N. Rega · V. Barone (✉)
Dipartimento di Chimica, Università di Napoli "Federico II",
Complesso Universitario Monte S. Angelo, via Cintia, 80126 Napoli, Italy
E-mail: baronev@unina.it

itself a chemically interesting one; moreover, it can also be regarded as a simple model to probe the general features of the carbonyl–water interaction, an issue of still wider chemical and biochemical interest. We have used Car-Parrinello molecular dynamics (CPMD) [14] simulations in aqueous solution (and, for comparison, in the gas phase) as starting points for the development of a modified force field based on the AMBER model [43], as well as for the validation of solvent/dynamical effects on spectroscopic parameters computed at the QM/PCM level on selected frames extracted from a classical molecular dynamics (MD) that employs the modified force field.

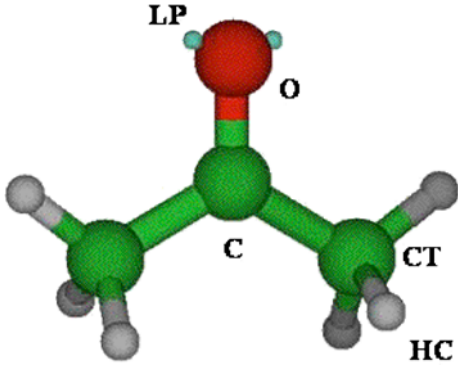

Fig. 1 Structure and atom labeling of the acetone molecule

2 Computational details

Quantum chemical calculations of structures and energies were performed with the GAUSSIAN 03 package [44]. Minimum-energy structures were obtained with the PBE functional [45] and a double ζ basis set including diffuse and polarization functions, namely 6-31+G(d,p) [46], while bulk solvent effects were taken into account by the PCM implicit solvation model [23–26]. Single point energy calculations and energy scans were carried out with the PBE0 functional [47], and different basis sets ranging from double and triple ζ sets from the Pople series, 6-31+G(d,p) and 6-311++G(2d,2p) [46], to the correlation consistent triple ζ basis set aug-cc-pVTZ [48].

The reference CPMD simulation was carried out with a parallel version [49] of the original Car-Parrinello code [50] implementing Vanderbilt pseudopotentials [51], using the PBE functional [45]. The equations of motion were integrated with a time step of 10 a.u. (0.242 fs) with an electron fictitious mass of 1,000 a.u.; core states were projected using "ultrasoft" pseudopotentials [51] and the wave-function was expanded in plane-waves up to an energy cut-off of 25 Ry. For the system in aqueous solution, the initial configuration was obtained starting from a previously equilibrated trajectory obtained for a constant-volume cubic supercell including 64 water molecules at a density of 1.00 g/cm^3 [52], by replacing a water molecule by acetone. The simulation in vacuo was performed, instead, starting from the optimized structure of acetone in a cubic cell with a side of 12.41 Å. The considered systems were equilibrated for 1.5 ps at 300 K, applying a Nosé thermostat [53], which enforces a canonical (NVT) ensemble. After equilibration, the trajectories of the systems were followed for 4.0 ps, during which statistical averages were taken. The average temperature during the simulations in vacuo and in aqueous solution was 312 and 320 K, respectively.

Molecular mechanics (MM) calculations and classical MD simulations were performed with the SANDER module of the AMBER 7 program [54]. Parameters for the carbonyl group were either taken from the original force field [43], or were modified as described in the next section. Partial atomic charges were obtained with the RESP approach [55], by fitting an electrostatic potential grid computed on the acetone molecule at the HF/6-31G(d) level of theory. Water molecules were described by the SPC/E [56] force field, which ensures a good description of the water structure and at the same time a low computational cost. Simulations were performed in a box containing one molecule of acetone and about 1,000 water molecules with a time step of 2.0 fs. After 140–200 ps of equilibration, the production phase (NVT) lasted for 200 ps more, at T=300 K. The geometry of the central acetone molecule was kept fixed, and the SHAKE algorithm was used to constrain all bonds of the solvent molecules [57].

NMR shieldings were obtained by the GIAO procedure [8–10], and electronic transition energies were computed by TD–DFT calculations [5–7]. The latest implementation [23–26] of the PCM [22] was used to account for bulk solvent effects, in combination with the UAHF set of atomic radii [25] and a non-equilibrium formulation for UV spectroscopic parameters [26].

3 Results and discussion

The structure and labelling of the acetone molecule are sketched in Fig. 1.

The aim of the present work was to parameterize an empirical force field in order to perform a reliable molecular dynamics simulation, which could reproduce the spectroscopic data computed starting from a CPMD simulation [32]. The first point was the definition of an acetone structure that was "CPMD-consistent"; to this aim, geometry optimizations were carried out with the same density functional employed in the Car-Parrinello dynamics (PBE) and the 6-31+G(d,p) basis set; solvent effects were taken into account by the PCM, with and without two explicit water molecules H-bonded to the carbonyl oxygen. The data collected in Table 1 clearly show that the PCM alone does not succeed in reproducing the CPMD data, whereas the PCM plus the inclusion of the two H-bonded water molecules leads to results in close agreement with the CP average data. During the whole CPMD simulations there are on the average two water molecules H-bonded to the carbonyl: the PCM succeeds in mimicking bulk solvent effects, but reproduces only partially strong and specific interactions in the first solvation shell. As a consequence,

Table 1 Geometrical parameters of acetone in vacuo and in aqueous solution obtained by different methods; distances in Angstroms (Å), angle in degrees (°)

	Exp./vacuum[a]	Calc./vacuum[b]	Calc./vacuum[c]	CPMD[d]	Calc./PCM[b]	Calc./2·H_2O+PCM[b]	Calc./2·H_2O+PCM[c]
C=O	1.210	1.229	1.207	1.25(0.01)	1.237	1.247	1.219
C—C	1.507	1.520	1.506	1.50(0.03)	1.511	1.502	1.498
C—H		1.102	1.091	1.11(0.04)	1.103	1.103	1.091
C—C=O	121.7	121.7	121.8	121(4)	121.6	121.1	121.3
C—C—C	116.7	116.6	116.4	117(5)	116.8	117.8	117.3

[a]Ref. [59], [b]PBE/6-31+G(d,p), [c]PBE0/aug-cc-pVTZ, [d]PBE/plane waves in aqueous solution with standard deviations in parentheses

Table 2 Energy differences (kcal/mol) for different orientations of the water molecules around the carbonyl plane in the Acetone $(H_2O)_2$ cluster

C–C=O$\cdots$ H_{water}	QM [a]	FF std.[b]	FF mod.[b]
0°	0.0	0.4	0.0
30°	1.0	0.0	1.5
60°	3.1	0.0	2.9
90°	4.0	0.2	6.0

[a]PBE0/6-311++G(2d,2p) single point calculations on PBE/6-31+G(d,p) geometries

[b]MM calculations on the same geometries with the standard or the modified force field

Table 3 Inter-molecular geometrical parameters of the acetone–$(H_2O)_2$ minimum-energy structure; distances in Angstroms (Å), angles in degrees (°)

	QM [a]	FF std.	FF mod.
$O_{acetone}\cdots H_{water}$	1.9	1.7	1.8
$O_{acetone}\cdots O_{water}$	2.9	2.7	2.8
$C=O_{acetone}\cdots H_{water}$	116.7	129.5	115.1
$O_{acetone}\cdots H–O_{water}$	162.1	177.3	170.6

[a]PBE/6-31+G(d,p)

PCM computations on the cluster formed by acetone and two water molecules lead to essentially complete account of the whole solvent effect. Thus, the acetone structure we choose for force field parameterization was that obtained from such a discrete/continuum approach, and it was kept fixed in all subsequent MM and MD calculations, both in vacuo and in solution.

The starting parameters we employed were taken from the standard AMBER force field [43], using "C" and "O" atom types for the carbonyl group, and "CT" and "HC" atom types for the methyl group. The most significant problems arising from the standard parameterization are related to the lack of any directional dependence for the H-bond interaction. Table 2 lists the energies computed for the system acetone–$(H_2O)_2$ at different (symmetric) orientations of the water molecules with respect to the acetone plane: it is clear that essentially no energetic differences are obtained by the standard force field. In order to avoid this kind of spherical symmetry around the acetone oxygen, and to achieve a correct energetic behavior when H-bonds depart from the acetone plane, we resorted to introducing two lone pairs. After some testing, an optimal position for the lone pairs was found at 0.45 Å from the oxygen and at a C=O. . .LP angle of 115°: this leads to a minimum-energy geometry of the acetone–$(H_2O)_2$ cluster that agrees closely with the reference QM minimum (Table 3). The introduction of lone pairs leads to the required directionality of the H-bond. Thus, for example, Fig. 2a shows a superposition of the water hydrogen atoms H-bonded to the acetone molecule extracted from MD simulations with the standard force field and with the modified parameters: the spurious spherical symmetry of the standard parameterization is correctly broken by the introduction of explicit lone pairs. At the same time, the $O_{acetone}$–H_{water} radial distribution function is in remarkable agreement with its CPMD counterpart (Fig. 2b). In order to achieve a correct energetic balance between acetone–water and water–water H-bonding, we also needed to modify the van der Waals parameters of the carbonyl oxygen. As a matter of fact, the arrangement of water molecules around acetone, and in particular hydrogen bonding to the carbonyl oxygen, is the other crucial structural parameter that needs to be quantified in the simulations. We adopted some simple and widespread geometrical criteria to identify H-bonds [58], namely:

$$\text{Distance}(O_{acetone}\cdots O_{water}) \leq 3.50\,\text{Å},$$
$$\text{Distance}(O_{acetone}\cdots H_{water}) \leq 2.60\,\text{Å},$$
$$\text{Angle}(H_{water}–O_{water}\cdots O_{acetone}) \leq 30°.$$

With this definition, the average number of water molecules H-bonded to carbonyl oxygen from CPMD is 2.1, whereas the standard AMBER force field leads to a significantly lower figure (1.6). As shown in Table 4, with our final parameterization the average number of H-bonds rises to 1.9, in much better agreement with the reference CPMD. During the modification of van der Waals parameters we were also guided by an analysis of the acetone–water interaction energies of the first and the second H-bond, in comparison with the water–water H-bond energy. Unlike QM computations, the standard force field predicts a binding energy for the second water molecule much weaker than for the first one, whereas the modified parameters restore the correct trend. In the last step of the parameterization, we also touched up the methyl group parameters, which in the standard force field are too repulsive. As a matter of fact, an energetic scan of the C=O$\cdots$ H_{water} angle for an acetone–(H_2O) cluster shows that the configuration space spanned by the standard force field is significantly narrower than it appears from QM calculation. For this reason, we chose to set to zero the van der Waals radii of the methyl hydrogen atoms, and included them into a modified "CT": this restores a close agreement with the QM trend (Fig. 3). The original AMBER parameters are

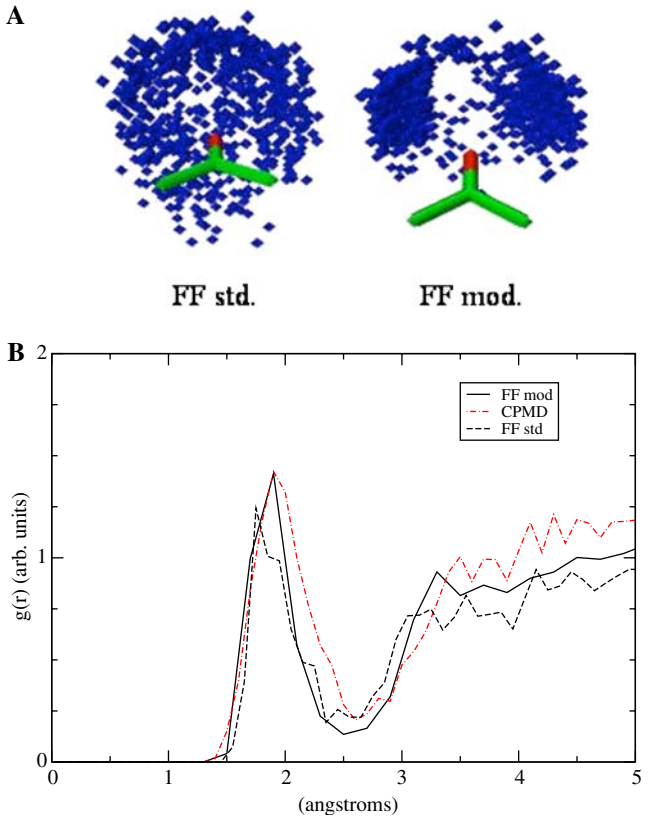

Fig. 2 Angular (A) and radial (B) distribution of water molecules around acetone resulting from MD runs employing the original and the reparameterized force field (see text for further details)

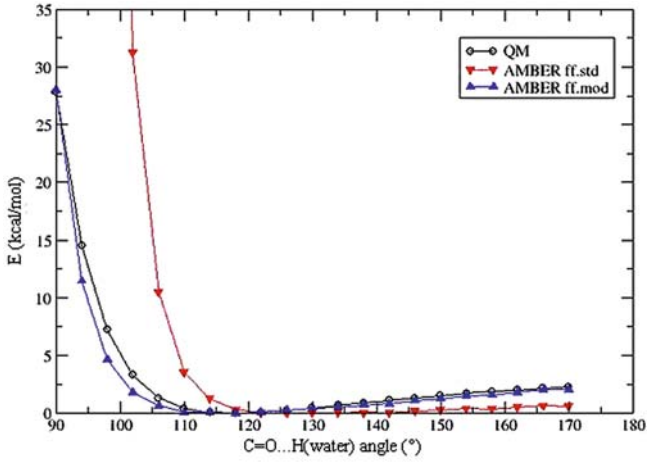

Fig. 3 Energy change as a function of the out-of-plane deviation of water molecules with respect to acetone (see text for further details)

compared in Table 5 to their counterparts optimized in the present study.

Eventually, the final validation of this modified AMBER force field concerned the calculation of spectroscopic parameters. We have recently shown that the overall solvent effect can be separated into a direct effect, issuing from molecular dynamics, and an indirect effect related to modifications of acetone geometrical parameters, which can be ob-

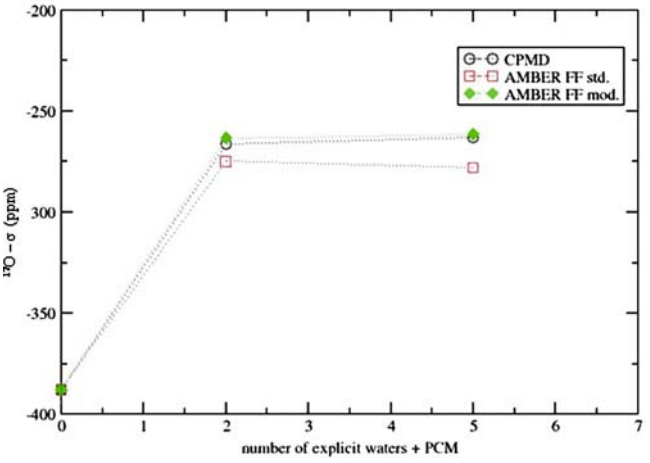

Fig. 4 Computed (PCM/GIAO/DFT) average ^{17}O absolute nuclear shielding as a function of the number (n) of explicit water molecules in the acetone–$(H_2O)_n$ clusters, extracted from different MD simulations

tained from geometry optimizations in vacuo and in solution [32]. Let us start the present analysis from direct solvent effects on the $n \rightarrow \pi^*$ excitation energy (UV parameter) and the ^{17}O nuclear shielding constant (NMR). From the MD trajectories we took about one hundred frames, equally spaced in time, and from each frame we extracted clusters containing the acetone molecule and a given number of the closest water molecules. Spectroscopic calculations were carried out on such acetone–$(H_2O)_n$ clusters, using PCM to account for the remaining part of the solvent. These calculations were performed by the PBE0 hybrid functional [47] with different basis sets: for the UV parameters, we adopted a 6-311++G(2d,2p) basis set on the carbonyl atoms, and a less expensive 6-31+G(d,p) basis set for the other acetone and water atoms, a combination that has already been successfully tested on the acetone-water system [31,32]. On the other hand, to compute NMR parameters we employed a triple ζ basis set, 6-311+G(d,p), which had been previously validated for this kind of calculations [11,12]. The acetone-$(H_2O)_n$/PCM results were compared to the data obtained at the same level of theory for the isolated acetone molecule at the same geometry: this procedure allows to estimate the direct solvent effect. The efficiency of the discrete/continuum approach and the accuracy of the proposed force field in comparison with the CPMD reference are well summarized in Fig. 4 (NMR parameters) and Fig. 5 (UV shifts). In both cases, two explicit water molecules, in combination with the PCM, are sufficient to completely account for the solvent effects: no significant difference is noted when the number of explicit water molecules is increased to five. A summary of the computed direct solvent shifts is reported in Table 6: overall, the modified force field performs very well, leading to an agreement with spectroscopic data derived from the CPMD reference that is much better than the one issuing from computations employing the standard force field. These results point out the strong relationship between force field accuracy and reliability of the computed spectroscopic data.

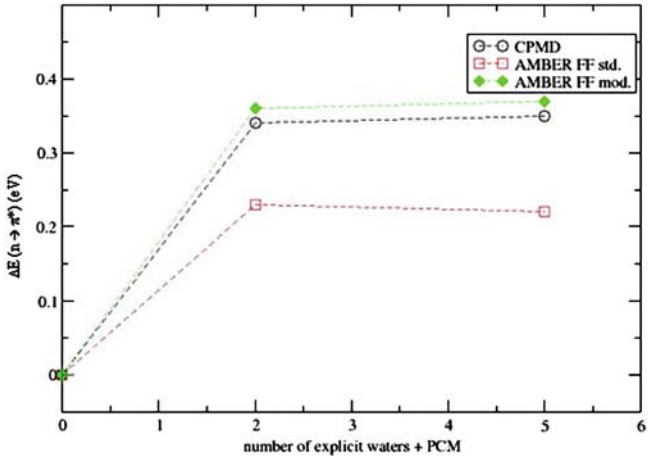

Fig. 5 Computed (PCM/TDDFT) average solvent shifts for the $n \rightarrow \pi^*$ transition as a function of the number (n) of explicit water molecules in the acetone–$(H_2O)_n$ clusters, extracted from different MD simulations

Table 4 Average number and distances of H-bonded water molecules during molecular dynamics simulations; distances in Angstrom (Å)

	CPMD	FF std.	FF mod.
Average number of H-bonds	2.1	1.6	1.9
$O_{acetone} \cdots H_{water}$	2.0	2.0	1.9
$O_{acetone} \cdots O_{water}$	2.9	2.8	2.9

Table 5 Acetone force field parameters

	Partial atomic charges		van der Waals parameters			
	FF std.	FF mod.	FF std.		FF mod.	
			R	ε	R	ε
C	0.6552	1.1414	1.9080	0.0860	1.9080	0.0860
O	−0.565	0.0000	1.6612	0.2100	1.7112	0.4600
LP	–	−0.3000	–	–	–	–
CT	−0.3250	−1.1372	1.9080	0.1094	1.9980	0.1879
HC	0.0933	0.2888	1.4870	0.0157	–	–

As mentioned above, direct comparison with experimental data requires an evaluation of indirect effects. To this end we have optimized (at the PBE0/aug-cc-pVTZ level) the geometry of acetone, either alone or in a cluster including two water molecules, taking into account, in the latter case, also bulk solvent effects by PCM. Furthermore, since PBE geometry optimizations in the gas phase overestimate the CO and CC bond lengths with respect to the closely matching PBE0 and experimental results [59] (see Table 1), we have added a further correction that corresponds to the difference between the spectroscopic parameters computed with PBE and PBE0 optimized geometries. All these contributions require standard QM geometry optimizations and are collected in Table 7. The overall results are now in remarkable agreement with experiment.

4 Concluding remarks

The present paper is devoted to an analysis of the different factors involved in the computation of reliable NMR and UV parameters of acetone in aqueous solution. Starting from TD–DFT or GIAO–DFT computations, both specific and long-range solvent effects play a role in determining the overall results. These contributions can be accounted for in the most effective way by mixed discrete/continuum solvent models, which can be used also in a dynamic context, resorting to Car-Parrinello or classical molecular dynamics. In the latter case, proper reparameterization of current force fields can be mandatory, since some spectroscopic parameters are sensitive not only to radial distribution functions, but also to angular distributions around non axially symmetric groups. Furthermore, spectroscopic parameters are much more demanding than structural parameters in terms both of scaling with the dimension of the QM system and of sophistication of the QM approach. Here again, continuum solvent models (PCM in the present case) come into play, since they allow to replace "on the fly" computations on the whole solute/solvent system by more refined computations carried out on smaller clusters embedded in a polarizable continuum, and averaged on a suitable number of frames. It is particularly gratifying in this connection that the number of explicit solvent molecules that must be included in order to obtain converged results is quite small.

In summary, the integrated computational tool consisting of the most recent hybrid density functionals, mixed discrete–continuum solvent models, and averaging from molecular dynamics simulations is becoming a valuable complement to experimental results. Furthermore, thanks to the implementation of all these items in user-friendly computer codes, this kind of analysis is or will shortly be feasible also by non-specialists, and for much larger molecules of biological and/or technological interest.

Table 6 Computed direct solvent shift on spectroscopic parameters, averaged over the MD simulations

Direct solvent shift	CPMD	FF std	FF mod
Δ E (n $\rightarrow \pi^*$)	0.33(0.02)	0.23(0.01)	0.36(0.01)
^{17}O-NMR σ	121.8(3)	113.0(2)	124.7(2)

Data are for clusters made up by the acetone molecule and the two water molecules closest to carbonyl oxygen extracted at regular times from the dynamic trajectories; Δ E (n $\rightarrow \pi^*$) in eV, ^{17}O-NMR σ in ppm
Values given in parentheses represent the standard errors on the means

Table 7 Different contributions on computed spectroscopic parameters obtained by the modified force field: Δ E (n $\rightarrow \pi^*$) in eV, ^{17}O-NMR σ in ppm

Direct solvent shift	Direct	Indirect	Correction	Total	Experiment
Δ E (n $\rightarrow \pi^*$)	0.36	−0.13	0.03	0.26	0.25[a]
^{17}O-NMR σ	124.7	−17.0	−27.0	80.0	75.5[b]

[a]Ref. [15], [b]Ref. [16]

Acknowledgements The authors thank the Italian Ministry for University and Research (MIUR) for financial support and the Bio-TekNet Regional Competence Center at Naples for computer facilities.

References

1. Goedecker S, Scuseria GE (2003) Comput Sci Eng 5:14
2. Scuseria GE (1999) J Phys Chem A 103:4782
3. Hohenberg P, Kohn W (1964) Phys Rev B 136:864
4. Kohn W, Sham L (1965) Phys Rev A 140:1133
5. Gross EKU, Kohn W (1985) Phys Rev Lett 55:2850
6. Stratmann RE, Scuseria GE, Frisch MJ (1998) J Chem Phys 109:8218
7. Casida ME (1994) In: Chong DP (ed) Recent advances in density functional methods (part I). World Scientific, Singapore, pp 155–192
8. Wolinski K, Hilton JF, Pulay P (1990) J Am Chem Soc 112:8251
9. Helgaker T, Jaszunski M, Ruud K (1999) Chem Rev 99:293
10. Cheeseman JR, Trucks GW, Keith TA, Frisch MJ (1996) J Chem Phys 104:5497
11. Crescenzi O, Correale G, Bolognese A, Piscopo V, Parrilli M, Barone V (2004) Org Biomol Chem 2:1577
12. Benzi C, Cossi M, Barone V (2004) Phys Chem Chem Phys 6:2557
13. Benzi C, Crescenzi O, Pavone M, Barone V (2004) Magn Res Chem 42:S57
14. Car R, Parrinello M (1985) Phys Rev Lett 55:2471
15. Schlegel HB, Millam JM, Iyengar SS, Voth GA, Daniels AD, Scuseria GE, Frisch MJ (2001) J Chem Phys 114:9758
16. Barone V (2005) J Chem Phys 122:014108
17. Ciofini I, Adamo C, Barone V (2004) J Chem Phys 121:6710
18. Barone V, Carbonniere P, Pouchan C (2005) J Chem Phys 122:224308
19. Persico M, Tomasi J (1994) Chem Rev 94:2027
20. Cramer CJ, Truhlar DG (1999) Chem Rev 99:2161
21. Tomasi J, Mennucci B, Cammi R (2005) Chem Rev 105:2999
22. Miertus S, Scrocco E, Tomasi J (1981) J Chem Phys 55:117
23. Cossi M, Scalmani G, Rega N, Barone V (2002) J Chem Phys 117:43
24. Scalmani G, Barone V, Kudin KN, Pomelli CS, Scuseria GE, Frisch MJ (2004) Theor Chem Acc 111:90
25. BaroneV, Cossi M, Tomasi J (1997) J Chem Phys 107:3210
26. Cossi M, Barone V (2000) J Phys Chem A 104:10614
27. Barone V, Crescenzi O, Improta R (2002) Quant Struct Act Relat 21:105
28. Improta R, Barone V (2004) Chem Rev 104:1231
29. Improta R, Barone V (2004) J Am Chem Soc 126:14320
30. Aquilante F, Cossi M, Crescenzi O, Scalmani G, Barone V (2003) Mol Phys 101:1945
31. Pavone M, Benzi C, De Angelis F, Barone V (2004) Chem Phys Lett 395:120
32. Crescenzi O, Pavone M, De Angelis F, Barone V (2005) J Phys Chem B 109:445
33. Bayliss NS, McRae EG (1954) J Phys Chem 58:1006
34. Hayes WP, Timmons CJ (1965) Spectrochim Acta 21:529
35. Waltz KN, Koerting CF, Kuppermann A (1987) J Chem Phys 87:3796
36. Suppan P (1990) J Photochem Photobiol 50:293
37. Tiffon B, Dubois JE (1978) Org Magn Res 11:295
38. Cossi M, Crescenzi O (2003) J Chem Phys 118:8863
39. Grozema FC, van Duijnen PT (1998) J Phys Chem A 102:7984
40. Coutinho K, Saavedra N, Canuto S (1999) J Mol Struct (Theochem) 466:69
41. Bernasconi L, Sprik M, Hutter J (2003) J Chem Phys 119:12417
42. Rohrig UF, Frank I, Hutter J, Laio A, VandeVondele J, Rothlisberger U (2003) Chem Phys Chem 4:1177
43. Cornell WD, Cieplak P, Bayly CL, Gould IR, Merz KM, Ferguson DM, Spellmayer DC, Fox T, Caldwell JW, Kollman PA (1995) J Am Chem Soc 117:5179
44. Frisch MJ et al. (2004) GAUSSIAN 03, revision C.02, GAUSSIAN, Inc., Pittsburgh
45. Perdew JP, Burke K, Ernzerhof M (1996) Phys Rev Lett 77:3865
46. Francl MM, Pietro WJ, Hehre WJ, Binkley J, Gordon MS, DeFrees DJ, Pople JA (1982) J Chem Phys 77:3654
47. Adamo C, Barone V (1999) J Chem Phys 110:6158
48. Dunning TH Jr (1989) J Chem Phys 90:1007
49. Giannozzi P, De Angelis F, Car R (2004) J Chem Phys 120:5903
50. Pasquarello A, Laasonen K, Car R, Lee C, Vanderbilt D (1992) Phys Rev Lett 69:1982
51. Vanderbilt D (1990) Phys Rev B 41:7892
52. Hetenyi B, De Angelis F, Giannozzi P, Car R (2004) J Chem Phys 120:8632
53. Nosé S (1984) J Chem Phys 81:511
54. Case DA et al. (2002) AMBER7, University of California, San Francisco
55. Bayly CI, Cieplak P, Cornell WD, Kollman PA (1993) J Phys Chem 97:10269
56. Berendsen HJC, Grigera JR, Straatsma TP (1987) J Phys Chem 91:6269
57. Miyamoto S, Kollman PA (1992) J Comput Chem 13:952
58. Ferrario M, Haughney M, McDonald IR, Klein ML (1990) J Chem Phys 93:5156
59. Hildebrand RL, Andreassen AL, Bauer SH (1970) 74:1586